Pre-print

A New Diagnostic Framework for Early Breast Lesion Identification

Spatial Thermal Imaging: A Physics-Based Inverse Thermal Approach for Morphological Reconstruction

Edward Jay, ThermEval.com

Abstract

Breast cancer mortality is strongly influenced by stage at diagnosis, emphasizing the need to identify developing lesions at the earliest detectable stages. This paper introduces a new diagnostic framework integrating morphological reconstruction with physiological interpretation to provide a coherent methodology for breast malignancy risk assessment. Spatial Thermal Imaging (STI), a physics-based inverse thermodynamic method, reconstructs the underlying thermal morphology from a standard thermal image.

The reconstructed morphology is evaluated using a structured set of physiological and morphological characteristics associated with pathological processes. Wavelet analysis evaluates the multi-scale structural coherence of each reconstructed characteristic, providing an objective measure of its reliability. Resulting confidence-modulated morphological findings are integrated with independent physiological assessment to generate the combined J-Index, representing the overall diagnostic assessment. The framework distinguishes confidence in lesion identification from confidence in pathological implication, producing structured reports comprising lesion localization, morphological classification, physiological assessment, confidence assessments, and supporting rationale.

In an observational dataset of 1,645 examinations, STI findings demonstrated approximately 93% concordance with MRI findings. These findings suggest STI is capable of reconstructing localized morphological features corresponding to pathology-confirmed lesions as small as approximately 1.5 mm, illustrating the potential value of morphology-based assessment beyond conventional modalities.

The STI J-Index framework employs conventional infrared breast images and is compatible with existing imaging systems and low-cost thermal cameras. Combined with explainable diagnostic reporting and continuing improvements in infrared imaging technology, the STI framework offers the potential for affordable, broader clinical adoption and prospective validation.

1. Introduction

Breast cancer is the most frequently diagnosed cancer in women worldwide[1]. Because mortality from the disease is strongly influenced by stage at diagnosis, affordable early detection through primary screening remains a central strategy for reducing mortality[2].

Current diagnostic imaging modalities generally infer the presence of underlying pathology by interpreting indirect manifestations of the underlying disease process. Although these approaches have demonstrated substantial clinical value, each possesses inherent limitations in the earliest stages of lesion development.

Early identification of developing breast lesions therefore requires more than detection alone. It requires a diagnostic framework capable of integrating independent structural and physiological evidence into a coherent clinical assessment. This paper presents such a framework.

The STI framework was motivated by the recognized limitations of classical breast thermography[3] as a stand-alone physiological assessment. Central to the proposed methodology is Spatial Thermal Imaging (STI), which reconstructs the thermal morphology required for meaningful morphological characterization. Together with physiological interpretation, these complementary assessments form the basis of an integrated diagnostic framework for early breast lesion identification.

STI provides the morphological reconstruction component of the proposed diagnostic framework. Rather than interpreting surface thermal patterns directly, diffusion-broadened thermal profiles are analyzed to reconstruct the underlying thermal morphology responsible for the measured surface thermal field. The reconstructed morphology is evaluated using seven morphological characteristics together with an independent physiological assessment associated with malignancy[4-8], which are integrated using Bayesian reasoning to assign regional morphological classifications (M0–M6). Each reconstructed morphological feature is subsequently evaluated using Wavelet analysis[9], which assesses its structural coherence and modulates its heuristic contribution. Quantitative parameters, including full width at half maximum (FWHM), spatial temperature gradients, and vascular intensity relationships, are further employed to estimate lesion dimensions, depth, and surrounding tissue density.

In an observational dataset of 1,645 examinations analyzed within a clinical thermal imaging reading service, cases flagged by STI for further investigation were referred for advanced imaging, most commonly magnetic resonance imaging (MRI). Approximately 93% of referred cases demonstrated concordance between MRI findings and the STI-identified abnormality. These findings indicate that STI can reconstruct localized morphological features corresponding to pathology-confirmed lesions as small as approximately 1.5 mm.

The same dataset also demonstrated the limitations of physiological assessment alone. Although high physiological classifications (TH4 and TH5) retain their well-established association with malignancy, approximately 11% of physiologically low-risk (TH2) examinations and 26% of equivocal (TH3) examinations were subsequently confirmed to harbor malignant lesions. These findings demonstrate that physiological assessment alone cannot reliably exclude developing malignant lesions, supporting the need for complementary morphology-based analysis.

By combining reconstructed morphological information with physiological thermal field evidence, STI provides two independent dimensions of diagnostic insight. Physiological thermal field characteristics are represented by a Physiological Index (P-Index), while reconstructed morphological structures are evaluated through a Morphology Index (M-Index). These two evidence streams are integrated through a logical decision framework to produce a composite J-Index representing overall malignancy risk.

2. Thermodynamic Basis of Morphological Reconstruction

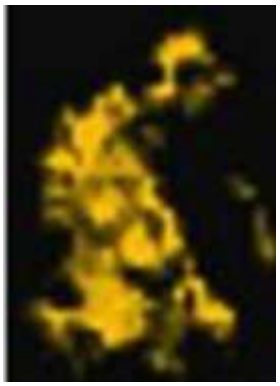

Figure 1. Representative STI morphological reconstruction illustrating recovery of thermal morphological fine structure. The reconstructed morphology demonstrates spatial organization, irregular geometry, and structural occupancy of the underlying heat-generating structures, providing the basis for subsequent quantitative morphological characterization.

The thermodynamic framework underlying STI is based upon the physical principles governing heat generation and diffusion within biological tissue[10]. Localized metabolic activity and angiogenic vascular recruitment associated with malignant development give rise to localized thermal fields within breast tissue. The resulting thermal field propagates through surrounding tissue and produces a measurable temperature distribution at the skin surface. Although this surface thermal image is often interpreted qualitatively, it contains recoverable information regarding the spatial distribution of the underlying physiological heat sources. STI treats the observed temperature field as a thermodynamic projection of these internal heat sources and applies reconstruction analysis to estimate their morphology and spatial characteristics.

During heat propagation, conductive diffusion broadens the thermal distribution. Analysis of this diffusion-modified structure provides information regarding the geometry of the originating heat source, including approximate lesion width, depth, and surrounding tissue characteristics.

Heat generated within biological tissue propagates primarily through conductive diffusion. As thermal energy moves from its source toward the skin surface, the spatial temperature distribution broadens due to diffusion and tissue heterogeneity. Consequently, the temperature pattern observed at the skin represents a diffusion-transformed projection of the underlying heat source rather than the source itself.

From an imaging perspective, this process may be viewed as a convolution between the subsurface heat source distribution and the thermal point spread function of tissue. Thermal diffusion therefore acts as a spatial low-pass filter that attenuates high-frequency spatial variations in the temperature field.

STI interprets thermal images as boundary solutions of the heat diffusion equation and applies inverse analysis to reconstruct the spatial characteristics of the heat sources responsible for the measured surface temperature distribution.

For purposes of conceptual development, STI treated thermal patterns as a set of virtual thermal wave fronts related to heat flow from internal physiological sources[11]. The virtual thermal wave concept was introduced solely as an interpretive visualization framework, not as a replacement for the underlying diffusion-based thermodynamic formulation. Within this conceptual framework, the temperature associated with each recorded pixel was interpreted as representing a virtual thermal wave propagating from localized subsurface heat sources[12]. This visualization provided an intuitive means of interpreting thermal propagation as structured wavefronts originating from localized physiological activity.

By reverse modeling the heat flow[13] measured at the breast surface, STI visually recreates the morphology and spatial organization of subcutaneous thermal sources associated with pathological development. This thermodynamic interpretation provides the basis for the STI reconstruction process described in the following section.

3. Morphological Reconstruction Methodology

STI reconstruction is based on analysis of the spatial structure of the surface thermal field rather than on isolated temperature measurements. Each recorded pixel represents a localized boundary expression of the underlying heat diffusion process, and meaningful interpretation therefore requires evaluation of the thermal field as a continuous spatial system.

In practice, STI analyzes local temperature gradients and neighborhood relationships within the thermal field to identify coherent thermodynamic structures associated with subsurface physiological heat sources. Because heat propagation in biological tissue is influenced by multiple variables—including tissue composition, vascular transport, and local thermal diffusivity—the exact forward solution cannot be uniquely inverted from surface temperature data alone. Instead, STI employs an iterative reconstruction approach in which thermodynamic parameters are varied within physiologically plausible limits to reveal stable morphological structures consistent with the observed surface thermal field[14].

During this process, the reconstruction is progressively refined through iterative evaluation of an effective thermodynamic transfer model (Figure 2). An initial coarse reconstruction establishes the approximate reconstruction regime, after which progressive refinement converges upon a definitive morphological representation consistent with the measured surface thermal field. This convergence reflects the point at which further refinement produces negligible change in the reconstructed morphology. AI-assisted wavelet analysis subsequently evaluates the multi-scale structural coherence of the definitive morphological representation and establishes an independent measure of confidence in the reconstructed field. The resulting reconstruction represents the most thermodynamically consistent morphological representation of the underlying physiological heat-source distribution.

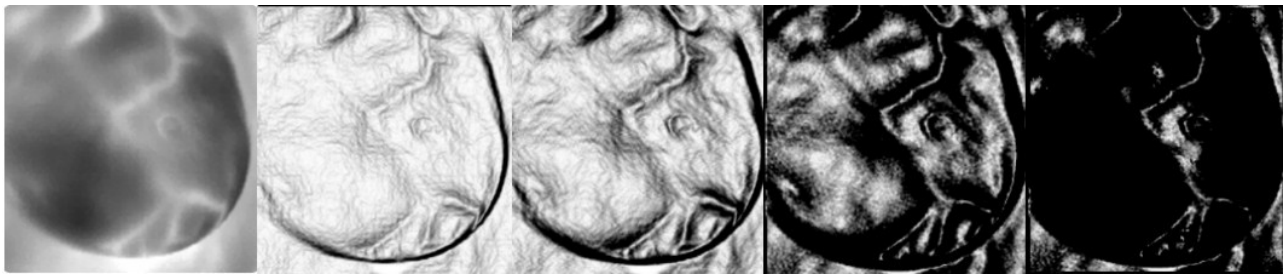

Figure 2. Representative progression of iterative STI morphological reconstruction from the measured surface thermal field to the definitive reconstructed morphology. Successive reconstruction iterations progressively refine the reconstructed morphology through evaluation of the thermodynamic transfer model. Convergence is achieved when further refinement produces negligible change in the reconstructed morphological structure, yielding the definitive representation used for subsequent quantitative characterization and confidence assessment.

3.1 Geometric Estimation of Reconstructed Heat Sources

The definitive morphological representation shown in Figure 2 identifies the presence and structural characteristics of reconstructed heat sources. However, a complete clinical characterization also requires estimation of their geometric properties. Lesion dimensions, depth, tissue density, and spatial location provide important contextual information for clinical interpretation and facilitate comparison with other imaging modalities.

Geometric characteristics of the reconstructed heat sources may be estimated from the diffusion-modified thermal field produced at the surface by heat originating from vascular or metabolic sources. This surface thermal field can be approximated by a Gaussian diffusion profile. This approximation permits characterization of the spatial thermal profile by its full width at half maximum (FWHM) and associated gradient properties[15].

Measurement of the FWHM of the diffusion-broadened thermal field provides an estimate of the lateral dimension of the originating heat source. Additional parameters, including spatial temperature gradients and the relative intensity of principal vascular structures, provide insight into the effective thermal diffusivity of the intervening tissue. Together, these relationships permit approximate estimation of lesion width, source depth, and surrounding tissue density characteristics. In the current implementation, depth estimation employs a first-order heuristic relationship between diffusion profile width and propagation distance, constrained by the estimated thermal characteristics of the intervening tissue. While this approximation provides useful geometric estimates, the precise functional relationship remains an area of ongoing refinement.

3.2 Resolution Stability of Morphological Reconstruction

The reconstructed morphology remains stable across thermographic image resolutions ranging from approximately 160 × 120 pixels to 640 × 480 pixels.

Higher-resolution sensors primarily improve the visual definition of fine vascular structures rather than materially altering the reconstructed morphology. This behavior is consistent with the physics of thermal diffusion, which limits the spatial bandwidth of thermal information reaching the skin surface.

Consequently, meaningful morphological reconstruction can be achieved using relatively low-cost thermographic sensors, substantially reducing instrumentation requirements while preserving diagnostic utility.

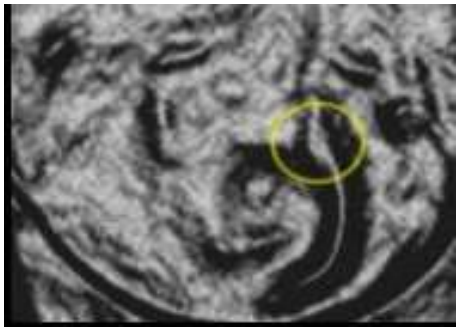

Figure 3. Representative example of a small reconstructed lesion obtained from a thermographic image acquired using a 160 × 120-pixel detector. The reconstructed lesion measures approximately 2 mm in diameter based on pixel measurements relative to the image width, illustrating the resolution stability of reconstructed morphology across thermographic image resolutions.

4. Morphological Interpretation Framework (M-Index)

STI analysis proceeds in two stages: thermodynamic reconstruction of the internal thermal field followed by morphological interpretation of the reconstructed heat-source morphology. The resulting morphological features are evaluated using the indicators described below to assign a Morphology Index (M-Index).

The reconstruction process produces a visualization of reconstructed morphology, including vascular architecture, localized heat-generating structures, lesion geometry, and their spatial organization within the breast. Interpretation then evaluates a set of morphological indicators associated with malignancy. The indicators described below were selected from established descriptions of the morphological characteristics most commonly associated with malignant tumors and adapted for evaluation within the STI reconstruction framework.

Eight morphological indicators (C1-C8) are assessed:

Indicator	Imaging Manifestation	Biological Interpretation
C1 – Vascular Association	Lesion occurs adjacent to or integrated with vascular structures	Malignant tumors recruit local blood supply
C2 – Focused vascularity	Localized concentration of Vessels surrounding a lesion	Angiogenic recruitment
C3 – Thermal state	Hyperthermia/Hypothermia relative to surrounding tissue	Increased metabolic activity
C4 – Geometry	Irregular or jagged lesion morphology	Structural disorganization of tumor growth
C5 – Tortuous Vessels	Curved, chaotic vascular morphology	Established tumor angiogenesis
C6 – Distorted vessels	Dilated or elongated vessel near lesion	Early vascular remodeling
C7 – Feeder/Drainage pattern	Presence of afferent and efferent vessels	Functional vascular network supplying lesion
C8 – Microthermal bubble formations	Small localized thermal maxima near developing vessels	Early biochemical activity associated with angiogenesis

Table 1. Morphological Indicators (C1-C8) Associated with Malignancy

Among these indicators, three have demonstrated particular diagnostic significance: tortuous vascular structures consistent with tumor-associated angiogenesis, irregular geometry indicating structural irregularity of tumor growth, and distorted vessels associated with early vascular remodeling.

Microthermal bubble formations were recognized following retrospective examination of cases initially interpreted as benign cystic structures but later confirmed as malignant. Subsequent analysis suggested that these localized thermal maxima frequently occur adjacent to developing vascular structures and may represent early biochemical activity associated with tumor angiogenesis.

Each characteristic is assigned a heuristic weight, k_i, reflecting its relative contribution to malignancy identification within the STI analytical hierarchy. These weights represent a working formalization of the qualitative diagnostic hierarchy developed through iterative clinical observation and case-based refinement.

As the STI case database expands, empirical calibration of these weighting factors against outcome-correlated data is anticipated.

Indicator	Diagnostic Role	Weight	Interpretation Role
C1 – Vascular association	Lesion plausibility	__	Vessel distance from lesion
C2 – Focused vascularity	Light	1	Local angiogenic recruitment
C8 – Bubble formations	Light	1	Early biochemical activity
C3 – Thermal anomaly	Supportive	1.5	Metabolic activity
C7 – Feeder-Drainer pair	Moderate	2	Functional vascular support network
C4 – Irregular geometry	Heavy	3	Structural irregularity of tumor growth
C5 – Tortuous vessels	Heavy	3	Classic tumor angiogenesis
C6 – Distorted vessels	Heavy	3	Early vascular remodeling

Table 2. Morphological Characteristics and Maximum Heuristic Contributions.

Although all morphological indicators contribute to lesion characterization, their relative diagnostic significance differs. STI therefore assigns each characteristic a maximum heuristic contribution reflecting its observed importance within the overall morphological assessment. In the current implementation, these maximum contributions are modulated by wavelet-derived measures of structural coherence and persistence.

Heavy weight (3.0)
C4, C5, and C6 represent the primary morphological and angiogenic indicators of malignancy in STI. Their simultaneous presence provides the strongest basis for elevated M-index assignment. C4 reflects the irregular lesion geometry produced by basal lamina penetration characteristic of invasive malignancy. C5 and C6 reflect pathological angiogenesis and nitric-oxide–mediated microcirculatory distortion, respectively, facilitating identification of nascent tumors that may not yet present a fully developed malignant vascular architecture.

Moderate weight (2.0)
C7 reflects identification of both afferent feeder and efferent drainage vessels, indicating establishment of a functional tumor vascular supply. Its presence represents a significant malignancy indicator but is weighted below the heavy characteristics because it may not yet be present in early-stage lesions.

Supportive/Conditional weight (1.5)
C3 represents thermal anomaly relative to surrounding tissue Marked hyperthermia (≥1 °C) is most commonly observed in inflammatory carcinoma and is absent in the majority of malignant lesions. Consequently, its absence is never penalizing, while its presence provides moderate positive support.

Light weight (1.0)
C2 and C8 provide supportive evidence but carry reduced standalone diagnostic weight due to benign overlap. Focused vascularity may occur with benign cystic structures, while microthermal bubble formations are subtle findings whose malignancy association, while biologically plausible through nitric-oxide–associated metabolic activity, remains supportive rather than determinative.

Lesion Identification Confidence (W)

Lesion identification confidence, W, is determined from six independently evaluated components describing the reliability of lesion identification and morphological characterization[16,17]. Five of these components (E, D, L, F, and I) are presently heuristic measures subject to future empirical calibration. The remaining component, B, incorporates biological plausibility through vascular association and is constrained by established pathological observations rather than purely heuristic *assessment.*

$$W = f(E, D, L, B, F, I)$$

where:

- **E** – coherent lesion existence;
- **D** – correct dominant-candidate selection;
- **L** – lesion-core localization;
- **B** – binding of C2–C8 to the identified lesion;
- **F** – stability of the reconstructed lesion field and geometric dimensions;
- **I** – image adequacy and freedom from confounding influences.

Parameter B quantifies the confidence that the reconstructed morphological characteristics (C2–C8) are correctly associated with the identified lesion. This association is governed by C1 vascular association, which represents the biological plausibility that the reconstructed morphology is supported by an appropriate vascular supply[18]. Pathological observations indicate that vascular support decreases rapidly as lesion-to-vessel separation increases and becomes negligible beyond approximately 3 mm. Accordingly, the contribution of B decreases continuously as lesion-vessel separation increases, approaching zero beyond approximately 3 mm, where vascular association is no longer considered biologically plausible.

For reporting purposes, lesion identification confidence is conveyed qualitatively using the descriptors Minimal, Low, Medium, Medium-High, High, and Maximum rather than as numerical percentages. These descriptors communicate the relative reliability of lesion identification without implying a statistically calibrated probability.

Having established confidence in lesion identification, the reconstructed morphological characteristics are subsequently evaluated within the STI interpretive framework to determine their collective implication of underlying pathology.

Wavelet Morphology Confidence

Wavelet analysis (WA) is a mathematical methodology for evaluating spatial fields simultaneously across multiple spatial scales. WA has become a standard analytical tool for multi-scale structural characterization in numerous scientific and engineering disciplines. Unlike conventional spatial filtering techniques, wavelet decomposition preserves spatial localization while simultaneously examining structural organization over multiple scales.

Applied to STI, wavelet decomposition allows reconstructed morphological features to be evaluated at multiple levels of resolution[19-20]. Morphological characteristics that remain spatially coherent across several decomposition scales are assigned greater confidence than isolated or scale-dependent features. Consequently, wavelet analysis provides an objective measure of the structural reliability of each reconstructed characteristic rather than a direct assessment of pathology.

The maximum heuristic contributions described above represent the potential diagnostic significance of each morphological characteristic. In practice, however, the contribution of each characteristic depends upon the structural coherence of the reconstructed morphology. STI therefore applies wavelet analysis to evaluate the multi-scale persistence and coherence of each characteristic, modulating its maximum heuristic contribution according to the confidence with which it is expressed within the reconstructed thermal field.

The wavelet-derived confidence values produced for each reconstructed characteristic subsequently contribute to the overall confidence framework described later. Thus, wavelet analysis serves as the quantitative bridge between morphological reconstruction and confidence estimation.

Morphology Index Computation

The confidence-modulated morphological characteristics are evaluated within a Bayesian-style interpretive framework to assign a regional Morphology Index (M-Index) ranging from M0 (no suspicious findings) to M6 (very high probability of malignancy)[22]. All wavelet-modulated morphological characteristics contribute to the raw morphology score.

Raw Morphology Score Computation

The raw morphology score is computed by summing the wavelet-modulated contributions of the seven morphological characteristics (C2–C8). Vascular association (C1) does not contribute

directly to the raw morphology score. Instead, it contributes to lesion identification confidence by providing a measure of biological plausibility.

Each morphological characteristic contributes its wavelet-modulated value to the raw morphology score:

Raw Morphology Score = C2 + C3 + C4 + C5 + C6 + C7 + C8

Each wavelet-modulated contribution, Ci, is computed as

$C_i = k_i * C_{i,max}$

where ki is the normalized wavelet confidence assigned to characteristic Ci, and Ci,max is its maximum heuristic contribution.

M-Index Mapping

The raw morphology score is mapped to the M-Index using the following threshold table. These threshold values represent the current operational STI classification and may be refined as additional outcome-correlated data become available.

Score S	M-Index	Description
0	M0	No morphological findings
0 - 2	M1	Minimal morphological findings
2.1 - 4.5	M2	Moderate morph. findings
4.6 - 7.0	M3	Substantial morph. findings
7.1 - 11	M4	Possible malignancy
11.1 - 13.4	M5	Likely malignant
13.5 - 14.5	M6	Highly probable malignancy

Table 3. M-Index Wavelet Confidence-Weighted Classification Thresholds

Pathological Implication Confidence, Wm

Pathological implication confidence, Wm, expresses the confidence that the identified lesion's collective morphology implies underlying pathology. It is distinct from lesion identification confidence, W, which evaluates whether the lesion has been reliably identified and characterized.

For M2 and M3:
Wm = Raw Morphology Score × W

For all other M-Index classifications:
Wm = Raw Morphology Score

If C1 < 0.25:
Wm = 0

For clinical reporting, Wm is expressed using qualitative confidence categories rather than numerical percentages, thereby communicating the relative strength of pathological implication without implying a statistically calibrated probability.

All seven wavelet-modulated morphological characteristics contribute to the raw morphology score. However, only characteristics whose normalized wavelet confidence exceeds 0.50 satisfy the criteria for inclusion in the narrative justification. Characteristics below this level remain part of the computation but are not individually cited as supporting pathological implication.

Limitations and Future Calibration

The weights and threshold values presented in this section represent heuristic parameters developed from the analytical hierarchy established through iterative clinical observation and case-based refinement. They have not yet been empirically calibrated using population-level outcome data.

The incorporation of wavelet-derived confidence modulation provides a bridge between purely heuristic weighting and future statistically optimized parameter estimation.

This developmental pathway is consistent with the historical evolution of many clinical scoring instruments. For example, the ACR BI-RADS[23] lexicon originated as an expert consensus classification system before undergoing subsequent prospective epidemiological validation.

The mathematical framework presented here is designed explicitly to support prospective calibration. As outcome-correlated malignancy data accumulate, statistical modeling approaches—such as logistic regression or likelihood ratio analysis applied to the characteristic set—may be used to replace the current heuristic weighting factors with empirically derived weighting coefficients. Threshold boundaries may then be refined to maximize diagnostic sensitivity and specificity for the target screening population.

Until such calibration is achieved, M-index values should be interpreted as probabilistic indicators within the STI analytical framework, consistent with the current FDA classification of STI as an experimental technique.

5. Physiological Interpretation Framework (P-Index)

Morphological characteristics describe the structural organization of reconstructed heat-generating regions. However, structural morphology alone does not fully characterize the underlying biological processes associated with lesion development. Because malignancy is fundamentally a physiological process expressed through structural change, evaluation of physiological activity provides complementary evidence beyond morphology alone.

The Physiological Index (P-Index) provides an independent assessment of the biological activity associated with the reconstructed morphology. Rather than evaluating structural characteristics, the P-Index considers physiological manifestations of malignant development, including vascular activity, metabolic response, tissue remodeling, and other thermophysiological indicators observable within the reconstructed thermal field. Together, these observations provide a quantitative estimate of the physiological activity of the reconstructed lesion.

The P-Index framework is based on the thermophysiological classification methodology originally developed by Michel Gautherie[24] through analysis of approximately 175,000 thermographic examinations of women diagnosed with breast cancer. These investigations identified the most frequently occurring and pathologically significant thermal field patterns statistically associated with malignancy.

Within the STI framework, physiological interpretation reflects the statistical likelihood of disease development associated with observed thermal field characteristics, independent of the spatial or morphological reconstruction analysis described previously. The STI physiological interpretation therefore preserves the epidemiological foundation of classical breast thermography while integrating it as an independent component within the overall STI diagnostic framework.

Physiological Signs

Consistent with this framework, the P-Index comprises five qualitative and ten quantitative thermopathological indicators describing characteristic physiological patterns observed in normal, inflammatory, and pathological breast tissue. The quantitative indicators represent measurable temperature differences associated with the qualitative observations. Each indicator contributes to the overall physiological assessment according to its frequency of occurrence and pathological significance.

Thermal Score and P-Index Classification

The total thermal score is obtained by summing the contributions of the qualitative and quantitative indicators present within the examination. The resulting score is classified into five ordinal physiological categories, shown in Table 4.:

P-Index	Thermal Field Character	Empirical Malignancy Incidence
P1	Normal	0%
P2	Borderline Normal	11%
P3	Borderline Abnormal	26%
P4	Abnormal	63%
P5	Markedly Abnormal	95%

Table 4. Physiological Index (P-Index) Classification.

These classification percentages were established empirically from longitudinal thermal studies and represent the proportion of cases within each physiological classification subsequently confirmed as malignant.

Within the STI diagnostic framework, the P-Index therefore provides an epidemiologically grounded physiological risk estimate that complements the morphology-based M-Index derived from reconstruction analysis.

6. J-Index Computation

Orthogonality of M-Index and P-Index

The M-index and P-index measure fundamentally different aspects of the breast thermal presentation:

The **M-Index** characterizes local spatial morphology reconstructed from the thermal field, including vascular architecture, thermal gradients, and lesion geometry within specific regions of interest.

The **P-Index** characterizes the global thermal field, reflecting the macroscopic physiological state of the breast, including systemic metabolic activity, vascular tone, and hormonal influence.

A focal lesion with a high M-Index may occur in a breast with a normal or low P-Index, particularly in early-stage malignancy where systemic metabolic perturbation has not yet manifested in the global thermal field. Conversely, a breast may present an elevated P-Index in the absence of a discrete focal lesion.

This functional orthogonality justifies the integration of the M-Index and P-Index into a combined diagnostic framework rather than treating either as a substitute for the other.

The J-Index is implemented as a lookup matrix that combines the M-Index and P-Index.

Let m ∈{1,2,3,4,5,6} denote the morphological M-Index level, , where the extended morphology category, **M6**, is assigned the value m=6, and let p ∈{0,1,2,3,4,5} denote the physiological P-Index level.

The combined risk classification, **J-Index**, is defined by the lookup matrix shown in Table 5.

P/M	0	M1	M2	M3	M4	M5	M6
P1	Minimal	Minimal	Minimal	Low	Moderate	Elevated	Severe
P2	Minimal	Low	Low	Moderate	Elevated	High	Severe
P3	Minimal	Low	Moderate	Elevated	Elevated	High	Severe
P4	Low	Moderate	Elevated	Elevated	High	High	Severe
P5	Low	Elevated	High	High	High	High	Severe

Table 5. J-Index Interpretation Matrix.

The J-Index classification comprises an ordered six-level diagnostic risk scale:

J = {Minimal, Low, Moderate, Elevated, High, Severe}

Boundary Conditions

The Severe classification represents the upper boundary condition of the J-Index:

J(p,6) = Severe for all p.

The M6 classification represents a complete malignant morphological profile and therefore produces the maximum J-Index classification regardless of the P-Index level. This reflects the clinical principle that a fully confirmed malignant spatial morphology constitutes the highest risk classification independent of global thermal field characteristics.

Properties of the J-Index Matrix

Several structural properties of the matrix are worth noting:

Monotonicity

The function J(m,p) is monotonically non-decreasing in both arguments. Increasing either the M-Index or the P-Index cannot reduce the resulting J-Index classification. It therefore follows that the J-Index constitutes an order-preserving integration of independent morphological and physiological evidence, ensuring that additional evidence from either domain cannot reduce the overall diagnostic classification.

Asymmetric Sensitivity

The matrix is intentionally more sensitive to increases in the **M-Index** than to increases in the **P-Index** at lower morphological levels.

A low M-Index is not disproportionately elevated by a high P-Index. For example, a **P5/M1** combination yields **Elevated** rather than High risk. This reflects the principle that abnormal surface thermal fields alone, without confirmable spatial morphological findings, do not constitute definitive evidence of malignancy.

Conversely, a high M-Index is not disproportionately suppressed by a low P-Index. For example, **P1/M4** produces **Moderate** risk. This reflects the principle that confirmed focal malignant morphology carries independent diagnostic significance even when the global thermal field appears relatively normal.

P5 Floor Effect

At P5, even M0 produces Low rather than Minimal risk. This reflects the strong epidemiological association between markedly abnormal physiological thermal fields and malignancy observed in longitudinal thermographic studies.

M6 Ceiling

The **Severe** condition is reached exclusively through the **M6** condition, reinforcing the diagnostic distinctiveness of a complete malignant morphological profile.

J-Index	Clinical Interpretation
Minimal	Combined findings do not support further investigation on thermal grounds alone
Low	Combined findings are mildly concerning; routine follow-up may be appropriate
Moderate	Combined findings warrant clinical attention; correlation with other imaging modalities recommended.
Elevated	Combined findings are significantly concerning; prompt clinical evaluation is indicated
High	Combined findings are strongly suggestive; urgent clinical evaluation and additional imaging are recommended
Severe	Combined findings represent the highest thermal risk level; immediate clinical evaluation is indicated.

Table 6. Clinical Interpretation of J-Index Levels

These interpretations are intended to assist the referring clinician and do not constitute a diagnosis. The J-Index, like the M-Index and P-Index individually, represents a probabilistic indicator within the STI analytical framework, consistent with the current FDA classification of STI as an experimental technique.

For practical clinical reporting, the combined outcome of the M-index, P-index, and J-index is expressed using a compact notation.

Notation

The combined assessment for any submitted case is expressed in the compact notation, e.g., P4/M4/High; P3/M6/Severe.

This notation provides a complete three-dimensional summary of the STI assessment in a compact, unambiguous format suitable for clinical reporting and database management.

Relationship to Prior Combined Indices

The J-index is conceptually related to prior attempts to combine surface thermographic classification with spatial imaging findings[27] but differs in two important respects.

First, the **M-index is derived from a formalized multi-characteristic spatial analysis** rather than from qualitative observer impression alone.

Second, the independence of the two inputs is structurally enforced. The P-Index is explicitly excluded from M-Index computation, preventing the double-counting that can occur when physiological thermal characteristics influence both physiological and morphological scoring simultaneously.

This separation ensures that physiological field interpretation and spatial morphological analysis remain analytically distinct components of the STI diagnostic framework.

7. Representative Clinical Report

The following excerpt illustrates the style and content of a representative report generated by the STI J-Index framework. It demonstrates how physiological assessment, morphological findings, lesion identification confidence, and pathological implication are integrated into a concise, clinically interpretable report[*].

Example 1. Representative STI J-Index Report Excerpt:

Left Breast Physiology: (P2) An atypical vascular pattern is seen at the upper half. It is concentrated at the upper-outer quadrant. Its maximum temperature is moderately higher (2.0°C) than the temperature of the same area on the opposite right breast, and mildly higher (1.0°C) than the mean temperature of the same left breast. The left breast is seen with global hyperthermia relative to the temperature of the adjacent sternal region. The temperature of the nipple/areola

[*] *Qualitative descriptors (e.g., **mildly**, **moderately**, and **significantly**) are standardized reporting terms derived from predefined quantitative thresholds and represent objective categorical classifications rather than subjective narrative descriptions.*

region of the left breast is significantly higher (1.5°C) than the temperature of the nipple/areola region of the right breast and moderately higher (1.5°C) than the mean temperature of the same left breast.

Left Breast Morphology: (M4) Internal visualization of the left breast demonstrates a lesion with significant morphological findings (possible malignancy) in the upper-outer quadrant at 1 o'clock, 23 mm from the nipple. The lesion measures 2.4 mm in width, 3.1 mm in height, and 1.8 cm deep, in medium-density tissue. This lesion demonstrates five of seven morphological signs associated with pathological implication, together with strong vascular association. Two additional morphological characteristics were observed but were insufficient to support the reporting criteria. Confidence in lesion identification is high. Confidence in the pathological implication of the lesion is elevated. The location of this lesion corresponds with the patient's reported symptom.

8. Future Development and Conclusions

The methodology presented here establishes a physics-based analytical framework for reconstructing, characterizing, and interpreting breast thermal fields. While the underlying methodological architecture has been established, several components—including wavelet-based confidence modulation, heuristic weighting factors, and J-Index transition boundaries—remain subject to empirical calibration as additional outcome-correlated clinical data become available.

The modular architecture of the STI framework permits refinement of individual computational components without altering the fundamental methodology. Future development will focus on optimization of wavelet confidence modulation, statistical calibration of heuristic weighting factors, and prospective refinement of the combined J-Index classification using pathology-correlated outcome data.

The next stage of STI development will consist of prospective clinical evaluation to determine diagnostic performance, optimize model calibration, and establish the clinical utility of the methodology for early breast lesion detection. Such evaluation will require collaboration with clinical investigators and access to appropriately designed pathology-correlated patient cohorts.

Because STI morphological reconstruction exhibits substantial stability across clinically relevant thermographic image resolutions, implementation does not depend upon specialized high-resolution instrumentation. The widespread availability of thermographic imaging systems capable of acquiring suitable thermal data therefore provides a practical foundation for future clinical evaluation and eventual implementation of the proposed diagnostic framework.

In conclusion, by integrating STI-based inverse thermodynamic reconstruction with morphology-based characterization, physiological interpretation, and combined risk assessment, the proposed diagnostic framework transforms breast thermal measurements into clinically meaningful morphological and physiological information, thereby supporting the objective of identifying developing breast lesions at their earliest detectable stages.

References:

1. Siegel RL et al. Cancer statistics, 2026. CA Cancer J Clin. 2026;76(1):e70043. doi:10.3322/caac.70043.

2. Charles Harding et al. Breast Cancer Screening, Incidence, and Mortality Across US Counties http://wilsonweb.physics.harvard.edu/publications/940ref.pdf.

3. Mashekova, A., et al. "Early detection of breast cancer using infrared technology." https://www.sciencedirect.com/science/article/pii/S2451904921003012

4. Konerding MA etal. Evidence for characteristic vascular patterns in solid tumors: Quantitative studies using corrosion casts. British Journal of Cancer. 1999;80(5-6):724.

5. Li C-Y et al. Initial Stages of Tumor Cell-induced Angiogenesis: Evaluation via Skin Window Chambers in Rodent Models. Journal of the National Cancer Institute. 2000;92(2):143-147, https://doi.org/10.1093/jnci/92.2.143.

6. P.Henro et al, Breast microcalcifications: The lesions in anatomical pathology, Diagnostic and Interventional Imaging Volume 95, Issue 2, February 2014, Pages 141-152.

7. Naoto Nishida et al, Angiogenesis in Cancer, Vascular Health Risk Management, 2006 Sep; 2(3): 213–219, https://www.ncbi.nlm.nih.gov/pmc/articles/PMC1993983/.

8. Luo, Q et al. Vasculogenic mimicry in carcinogenesis and clinical applications. J Hematol Oncol 13, 19 (2020), https://doi.org/10.1186/s13045-020-00858-6.

9. "Wavelet Transforms and Time-Frequency Signal Analysis;" Edited by Lokenath Debnath. https://link.springer.com/book/10.1007/978-1-4612-0137-3

10. Ying-Ze Wang et al. Heat transport properties within living biological tissues with temperature-dependent thermal properties; https://iopscience.iop.org/article/10.1088/1674-1056/ac6b29

11. R.K.Sahoo. Propagation of Thermal Waves with Lateral Heat Transfer, https://doi.org/10.1016/0011-2275(94)90170-8.

12. P. Burgholzer et al; Three-dimensional Thermographic Imaging Using a Virtual Wave Concept, https://arxiv.org/ftp/arxiv/papers/1610/1610.00868.pdf.

13. Martin Zálešák et al. Solution approaches to inverse heat transfer problems with and without phase changes: A state-of-the-art review; https://www.sciencedirect.com/science/article/abs/pii/S0360544223013683

14. Leigh Stanger et al. Reconstruction of Microscopic Thermal Fields from Oversampled Infrared Images in Laser-Based Powder Bed Fusion; https://pmc.ncbi.nlm.nih.gov/articles/PMC8309808/

15. Brown, B.S., et al. (2022). Influence of Thermal Diffusion on the Spatial Resolution of Thermal Imaging. https://par.nsf.gov/servlets/purl/10359552

16. Zhang, H., et al. (2024). “Artificial intelligence-based classification of breast lesions from imaging data: Diagnostic accuracy and confidence measures.”

https://pmc.ncbi.nlm.nih.gov/articles/PMC11093474/.

17. “Breast Lesion Detection Using Weakly Dependent Customized Features and Machine Learning Models with Explainable Artificial Intelligence":
https://www.mdpi.com/2313-433X/11/5/135

18. N. Weidner et al. “Current pathologic methods for measuring intratumoral microvessel density as a prognostic factor in breast Cancer"

https://pubmed.ncbi.nlm.nih.gov/8534865/

19. Rhif, M., et al. (2019). "Wavelet Transform Application for/in Non-Stationary Time-Series Analysis."
https://www.mdpi.com/2076-3417/9/7/1345

20. Hu, W., et al. (2016). "Multiple wavelet coherence for untangling scale-specific and localized features of transient processes." https://hess.copernicus.org/articles/20/3183/2016/hess-20-3183-2016.pdf

21. Ji, K., et al. (2026). "Nonstationary spatial coherence modeling via wavelet packet transform and deep sequence learning."
Link: https://www.sciencedirect.com/science/article/pii/S1093968726030628

22. Burnside, E.S., et al (2006). “Bayesian network to predict breast cancer risk of malignancy.” *Radiology*, https://pubmed.ncbi.nlm.nih.gov/16926323/.

23. Metaxa, L., et al. (2019). The UK RCR 5-point breast imaging system or BI-RADS; which is better? PMC, https://pmc.ncbi.nlm.nih.gov/articles/PMC6849664/

24. Breast Thermography and Cancer Risk Prediction MICHEL GAUTHERIE, PHD,' AND CHARLES M. GROS, MD; https://www.wellbloomington.com/wp-content/uploads/2014/01/Gautherie-et-al-1980-Cancer.pdf